



# Local structural ordering in low-temperature-grown epitaxial $\text{Fe}_{3+x}\text{Si}_{1-x}$ films on Ge(111)

K. Hamaya\*

*Department of Electronics, Kyushu University, 744 Motoooka, Fukuoka 819-0395, Japan and  
PRESTO, Japan Science and Technology Agency, Sanbancho, Tokyo 102-0075, Japan*

T. Murakami and S. Yamada

*Department of Electronics, Kyushu University, 744 Motoooka, Fukuoka 819-0395, Japan*

K. Mibu

*Nagoya Institute of Technology, Nagoya, Aichi 466-8555, Japan*

M. Miyao

*Department of Electronics, Kyushu University, 744 Motoooka, Fukuoka 819-0395, Japan and  
CREST, Japan Science and Technology Agency, Sanbancho, Tokyo 102-0075, Japan*

(Received 4 January 2011; revised manuscript received 27 February 2011; published 14 April 2011)

For exploring group-IV semiconductor spintronics with ferromagnetic Heusler compounds, we study the local structural ordering of the stoichiometric  $\text{Fe}_3\text{Si}$  and off-stoichiometric  $\text{Fe}_{3.2}\text{Si}_{0.8}$  films epitaxially grown on Ge(111) at a very low temperature of 130 °C. Analyzing their  $^{57}\text{Fe}$  Mössbauer spectra, we can discuss the site occupation of Fe atoms in the films grown directly on a semiconductor substrate, where the influence of the interfacial reactions between  $\text{Fe}_3\text{Si}$  or  $\text{Fe}_{3.2}\text{Si}_{0.8}$  and Ge on the Mössbauer spectra is minimized. As a result, we can quantitatively obtain the local degree of the  $\text{D0}_3$  ordering ( $\sim 67\%$ ) for the as-grown stoichiometric films, whereas we can not see the structural ordering for the as-grown off-stoichiometric films. Comparing the analytic data between as-grown and annealed films, we find that the postannealing can act effectively on the improvement of the structural ordering only for the off-stoichiometric films.

DOI: [10.1103/PhysRevB.83.144411](https://doi.org/10.1103/PhysRevB.83.144411)

PACS number(s): 75.50.Bb, 75.25.-j, 75.70.Ak, 76.80.+y

## I. INTRODUCTION

For the combination of high-performance spintronic devices with semiconductor technologies, the fabrication of highly ordered ferromagnetic Heusler compounds on semiconductor substrates is required.  $\text{D0}_3$ -type  $\text{Fe}_3\text{Si}$ , which is one of the ferromagnetic Heusler compounds, has a high Curie temperature of  $\sim 800$  K<sup>1</sup> and relatively high spin polarization of  $\sim 0.45$ , even for thin-film samples.<sup>2</sup> For spintronic applications, many researches have so far demonstrated epitaxial growth of  $\text{Fe}_3\text{Si}$  thin films on semiconductor substrates such as GaAs,<sup>2-4</sup> Si,<sup>5-7</sup> and Ge,<sup>8</sup> and their magnetic properties and structural characteristics have been investigated in detail.<sup>2-4,9-15</sup> The obtained knowledge of high-quality formation of  $\text{Fe}_3\text{Si}$  thin films can be expanded to the crystal growth techniques of half-metallic Heusler compounds with highly ordered structures.<sup>16-18</sup>

However, in general, it is very difficult to grow highly ordered  $\text{Fe}_3\text{Si}$  films directly on semiconductor substrates at high growth temperatures because of the easy occurrence of the interfacial reaction and atomic interdiffusion between  $\text{Fe}_3\text{Si}$  and semiconductors.<sup>13,15,19,20</sup> In fact, the epitaxially grown  $\text{Fe}_3\text{Si}$  films on GaAs showed relatively large influence of the interdiffusion at the  $\text{Fe}_3\text{Si}/\text{GaAs}$  interface on the structural ordering examined by the measurements of  $^{57}\text{Fe}$  conversion electron Mössbauer spectroscopy (CEMS).<sup>15</sup> Recently, we demonstrated epitaxial growth of  $\text{Fe}_3\text{Si}$  thin films on group-IV semiconductors Si and Ge by using low-temperature molecular beam epitaxy (LTMBE), and the heterointerfaces between  $\text{Fe}_3\text{Si}$  and Si or Ge were, surprisingly, atomically flat.<sup>7,8,13,14</sup> These results imply that we started to establish one of the key

technologies for group-IV semiconductor spintronics using Heusler compounds.<sup>21</sup>

Up to now, we have clarified that the growth temperature should be lower than 200 °C for obtaining high-quality epitaxial  $\text{Fe}_3\text{Si}$  layers<sup>7,8</sup> and the exact stoichiometry is quite important to realize highly axial orientation.<sup>13</sup> However, we have not obtained any information on the correlation between magnetic properties and structural characteristics for epitaxial  $\text{Fe}_{3+x}\text{Si}_{1-x}$  films grown on group-IV semiconductors yet. In particular, the degree of the structural ordering of their epitaxial  $\text{Fe}_{3+x}\text{Si}_{1-x}$  films has not been elucidated because we could not separate the (111) superlattice reflection peak of the  $\text{Fe}_3\text{Si}$  layer from the large diffraction peak of the Si(111) or Ge(111) substrate in x-ray diffraction measurements. Furthermore, understanding of fundamental features for obtaining highly ordered  $\text{Fe}_3\text{Si}$  films is basically important so as to form other Heusler compounds with highly ordered structures on Si and/or Ge.<sup>17</sup>

In this paper, we explore the structural ordering of the epitaxial  $\text{Fe}_{3+x}\text{Si}_{1-x}$  films grown on Ge(111) by  $^{57}\text{Fe}$  CEMS measurements. Unlike  $\text{Fe}_3\text{Si}$  films on GaAs,<sup>15</sup> we can observe the Mössbauer spectra with almost no influence of interfacial reactions between  $\text{Fe}_{3+x}\text{Si}_{1-x}$  and Ge. Comparing two different epitaxial films with stoichiometric ( $x = 0$ ) and off-stoichiometric ( $x = 0.2$ ) chemical compositions, we study the detailed information on the correlation between magnetic properties and structural characteristics. The structural ordering and saturation magnetization of the epitaxial  $\text{Fe}_{3+x}\text{Si}_{1-x}/\text{Ge}$  are strongly affected by their chemical compositions. It should be noted that we can discuss the

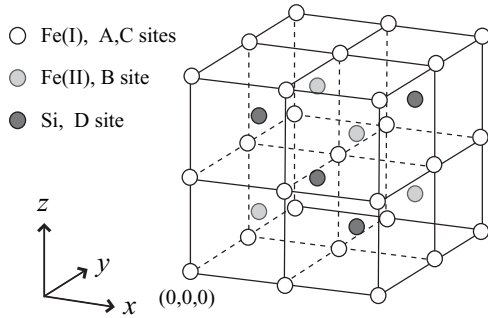


FIG. 1. Schematic diagram of  $D0_3$ -type  $\text{Fe}_3\text{Si}$ . There are two distinct crystallographic and magnetic Fe sites, i.e., Fe(I), occupying the (A,C) sites coordinated with four Fe atoms and four Si atoms, and Fe(II), occupying the B site surrounded by eight Fe atoms.

site occupation of Fe atoms for both as-grown and annealed samples, revealing that  $\sim 67\%$  of the local degree of the  $D0_3$  ordering can be obtained only for the as-grown stoichiometric film, but that an improvement of the structural ordering by the postannealing can be seen only for the off-stoichiometric film.

## II. IDEAL $D0_3$ -ORDERED STRUCTURE

Prior to the fabrication of thin-film samples and their characterizations, the structural and magnetic properties for general bulk samples are explained. The crystal structure of the ideal  $D0_3$ -ordered  $\text{Fe}_3\text{Si}$  is schematically illustrated in Fig. 1. There are four crystal sites denoted as A(0,0,0),  $B(\frac{1}{4}, \frac{1}{4}, \frac{1}{4})$ ,  $C(\frac{1}{2}, \frac{1}{2}, \frac{1}{2})$ , and  $D(\frac{3}{4}, \frac{3}{4}, \frac{3}{4})$  in Wyckoff coordinates.<sup>1</sup> In this binary Heusler structure, we can see three Fe sites, i.e., (A,C) site and B site, and one Si site, i.e., D site, where the A and C sites are equivalent in the ideal  $D0_3$ -ordered structure. Thus, there are two distinct crystallographic and magnetic Fe sites: Fe(I), occupying the (A,C) sites coordinated with four Fe atoms and four Si atoms, and Fe(II), occupying the B site surrounded by eight Fe atoms.<sup>1,22</sup> Experimental assignments revealed that the local magnetic moment of Fe(I) yields  $1.35 \mu_B/\text{atom}$  while that of Fe(II) reaches  $2.20 \mu_B/\text{atom}$ .<sup>22</sup> The calculated local magnetic moment of Fe(II) always becomes larger than that of Fe(I),<sup>23–27</sup> where Bansil *et al.* theoretically claimed that there is a difference in the down-spin states between Fe(I) and Fe(II), with electrons occupied or unoccupied, respectively, leading to the reduction in the net magnetic moment of Fe(I) compared with Fe(II).<sup>26</sup> However, if the Si nearest neighbors for these Fe sites increase due to off-stoichiometry and disorder, the average magnetic moment can be varied markedly.<sup>28–31</sup>

## III. SAMPLE PREPARATION AND CHARACTERIZATIONS

In this study, 25-nm-thick  $\text{Fe}_{3+x}\text{Si}_{1-x}$  thin films were grown on Ge(111) by LTMBE at  $130^\circ\text{C}$ ,<sup>7,8,13,14,17,21</sup> where we coevaporated Fe and Si using Knudsen cells. In order to change the chemical compositional ratio of Fe to Si, the growth rate of Fe was tuned by adjusting the cell temperature. For comparison, we intentionally grew two different thin-film samples, i.e., stoichiometric  $\text{Fe}_3\text{Si}$  ( $x = 0$ ) and off-stoichiometric  $\text{Fe}_{3.2}\text{Si}_{0.8}$  ( $x = 0.2$ ). During the growth, we observed *in situ* reflection high-energy electron diffraction (RHEED) patterns of the  $\text{Fe}_{3+x}\text{Si}_{1-x}$  layers. For both samples,

the RHEED patterns exhibited symmetrical streaks, indicating good two-dimensional epitaxial growth. Postannealing was also carried out at  $T_A = 200, 250, 300, 350, 400,$  and  $450^\circ\text{C}$  for 30 minutes in  $\text{N}_2$  atmosphere to study the effect of the annealing on the structural ordering.

Their crystal structures were characterized by means of x-ray diffraction (XRD), cross-sectional transmission electron microscopy (TEM), and nanobeam electron diffraction (NED).<sup>7,8,13,14</sup> Since there was almost no lattice mismatch between  $\text{Fe}_3\text{Si}$  and Ge and the diffraction peak intensity of Ge(111) was strong, the diffraction peaks could not be separated in  $\theta - 2\theta$  XRD measurements. However, there was no peak due to other  $\text{Fe}_x\text{Si}_y$  compounds. Magnetic properties and  $^{57}\text{Fe}$  Mössbauer spectra were measured with a vibrating sample magnetometer (VSM) and conversion electron Mössbauer spectroscopy, respectively, at room temperature. To enhance the detectability of the CEMS measurements, we enriched  $^{57}\text{Fe}$  nuclei to 20% in the Knudsen cell of the Fe source.

## IV. STRUCTURES AND MAGNETIC PROPERTIES

To examine the effect of chemical composition on the crystal structures and heterointerfaces, we observed cross-sectional TEM images for as-grown  $\text{Fe}_{3+x}\text{Si}_{1-x}$  films. Figures 2(a) and 2(b) show high-resolution TEM images of  $\text{Fe}_3\text{Si}/\text{Ge}(111)$  and  $\text{Fe}_{3.2}\text{Si}_{0.8}/\text{Ge}(111)$  interfaces, respectively. For  $\text{Fe}_3\text{Si}/\text{Ge}(111)$  [Fig. 2(a)], we can clearly see an atomic-scale abruptness with no interfacial fluctuation, as also shown in our previous works,<sup>7,8,13,14</sup> while, for  $\text{Fe}_{3.2}\text{Si}_{0.8}/\text{Ge}(111)$  [Fig. 2(b)], we can see structural fluctuations of a few monolayers at the interface. By these direct

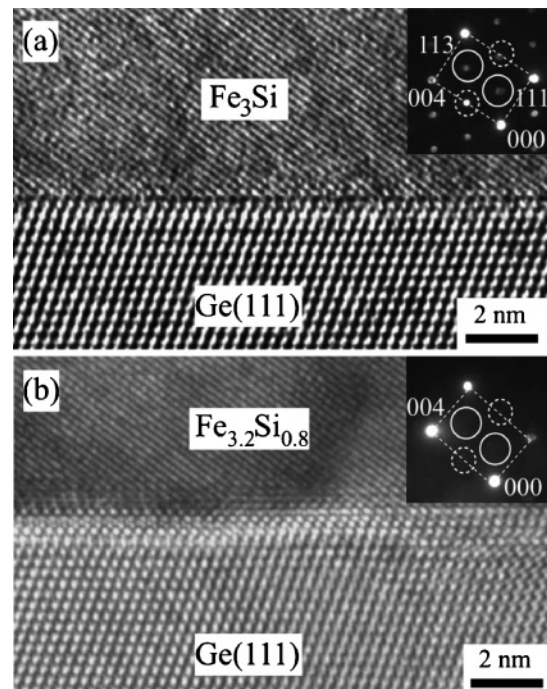


FIG. 2. Cross-sectional TEM images of (a)  $\text{Fe}_3\text{Si}/\text{Ge}(111)$  and (b)  $\text{Fe}_{3.2}\text{Si}_{0.8}/\text{Ge}(111)$ . The insets show nanobeam electron diffraction patterns for each  $\text{Fe}_{3+x}\text{Si}_{1-x}$  film near the interface. The zone axis is parallel to the  $[1\bar{1}0]$  direction.

observations, a small influence of chemical composition on the quality of the  $\text{Fe}_{3+x}\text{Si}_{1-x}/\text{Ge}(111)$  heterointerfaces can be confirmed. However, we can infer that the chemical reactions at the interface are not observed and the atomic interdiffusion is probably minimized even for  $\text{Fe}_{3.2}\text{Si}_{0.8}/\text{Ge}(111)$ . We have also observed NED patterns of the  $\text{Fe}_{3+x}\text{Si}_{1-x}$  films near the interface for  $\text{Fe}_3\text{Si}/\text{Ge}(111)$  and  $\text{Fe}_{3.2}\text{Si}_{0.8}/\text{Ge}(111)$ , as shown in the inset of Figs. 2(a) and 2(b), respectively. It should be noted that a clear difference in the ordering of the crystal structure is identified. For  $\text{Fe}_3\text{Si}/\text{Ge}(111)$ , there are  $\langle 111 \rangle$  and  $\langle 113 \rangle$  superlattice reflections resulting from the presence of  $\text{D0}_3$ -ordered structures (solid circle), together with clear superlattice reflections for  $\text{B2} + \text{D0}_3$  structures (dotted circles). By contrast, for  $\text{Fe}_{3.2}\text{Si}_{0.8}/\text{Ge}(111)$ , we can not see the above reflections, indicating that there are only  $\text{A2}$  disordered structures near the interface. From these structural characterizations, we conclude that the stoichiometry crucially affects the structural ordering of  $\text{Fe}_{3+x}\text{Si}_{1-x}$  films grown in our LTMBE conditions.

Figure 3(a) shows field-dependent magnetization ( $M-H$ ) curves measured at 300 K for  $\text{Fe}_3\text{Si}$  and  $\text{Fe}_{3.2}\text{Si}_{0.8}$  films, where the applied field direction is parallel to the magnetic easy axis in the film plane. The clear difference in saturation magnetization ( $M_S$ ) is observed, and  $M_S$  is estimated to be  $\sim 858$  and  $\sim 1155$   $\text{emu}/\text{cm}^3$  for the  $\text{Fe}_3\text{Si}$  and  $\text{Fe}_{3.2}\text{Si}_{0.8}$  films, respectively. Note that  $M_S$  for the  $\text{Fe}_{3.2}\text{Si}_{0.8}$  film is quite higher than that for the  $\text{Fe}_3\text{Si}$  film. This feature is similar to that for bulk samples and epitaxial-film samples reported.<sup>1,3,4</sup> We also conducted postannealing at various annealing temperatures ( $T_A$ ) and measured  $M_S$  for all the annealed samples. We

summarize the  $M_S$  versus  $T_A$  plot for the  $\text{Fe}_3\text{Si}$  and  $\text{Fe}_{3.2}\text{Si}_{0.8}$  films in Fig. 3(b). With increasing  $T_A$ , the  $M_S$  values gradually decrease for both series of samples, and significant reductions in  $M_S$  can be seen at  $T_A = 450$  °C and 400 °C for  $\text{Fe}_3\text{Si}$  and  $\text{Fe}_{3.2}\text{Si}_{0.8}$ , respectively. As discussed in our previous works,<sup>13,14</sup> the reductions in  $M_S$  at  $T_A = 400 \sim 450$  °C were attributed to the interfacial reactions between  $\text{Fe}_{3+x}\text{Si}_{1-x}$  and Ge and/or atomic interdiffusion. On the other hand, we could not observe them by means of TEM and NED for both series of samples below  $T_A = 350$  °C. That is to say, even if there is almost no observable interfacial reaction,  $M_S$  can decrease from  $\sim 858$  and  $\sim 1155$   $\text{emu}/\text{cm}^3$  to  $\sim 760$  and  $\sim 1033$   $\text{emu}/\text{cm}^3$  for  $\text{Fe}_3\text{Si}$  and  $\text{Fe}_{3.2}\text{Si}_{0.8}$ , respectively. These features are also consistent with those in our previous work.<sup>14</sup> In the last section, we use the annealed samples at  $T_A = 350$  °C to investigate the effect of postannealing on the local structural ordering and magnetic environment.

## V. SITE OCCUPATION

We have investigated the magnetic environments around the Fe sites of the  $\text{Fe}_{3+x}\text{Si}_{1-x}$  films epitaxially grown on Ge(111) by means of  $^{57}\text{Fe}$  Mössbauer spectroscopy in order to comprehend the effects of stoichiometry on the above structural and magnetic properties. If the ideal  $\text{D0}_3$ -ordered  $\text{Fe}_3\text{Si}$ , as depicted in Fig. 1, is formed, we can detect the two different surroundings of Fe atoms with two distinct hyperfine magnetic fields.<sup>15,28–32</sup> Figures 4(a) and 4(b) show the  $^{57}\text{Fe}$  Mössbauer spectra of the as-grown epitaxial  $\text{Fe}_3\text{Si}$  and  $\text{Fe}_{3.2}\text{Si}_{0.8}$  films, respectively, measured at room temperature. Evident sextet patterns, typical for magnetically ordered systems, are obtained for both samples. Note that the spectrum of the epitaxial  $\text{Fe}_3\text{Si}$  film on Ge(111) [Fig. 4(a)] is quite similar to that for the epitaxial  $\text{Fe}_3\text{Si}$  films on MgO reported by Krumme *et al.*,<sup>15</sup> but is quite different from that for the epitaxial  $\text{Fe}_3\text{Si}$  films on GaAs(001).<sup>15</sup> This fact indicates that the sample quality of our thin films is as good as the films grown on MgO, which is a well-established substrate that enables us to demonstrate a magnetically clean interface for the growth of  $\text{Fe}_3\text{Si}$  films.<sup>15</sup> Thus, we can discuss the site occupation of Fe atoms for epitaxial  $\text{Fe}_{3+x}\text{Si}_{1-x}$  films grown on Ge(111). Each spectrum in Fig. 4 was fitted with the next seven magnetic environments, by referring to the previous article,<sup>28</sup> including Fe(I) and Fe(II) sites in the ideal  $\text{D0}_3$ -ordered  $\text{Fe}_3\text{Si}$ . Here, we define the site number  $n$  from 1 to 7 as follows. First, the sites 1 and 2 with the hyperfine magnetic field of 20.0 and 31.3 T are Fe(I) and Fe(II), with four- and eight-nearest-neighbor Fe atoms, respectively, where the site with seven neighboring Fe atoms can not be distinguished from the site 2. Next, the site 3 with 32.8 T represents the Fe atoms in an  $\text{A2}$ -type Fe phase with eight-nearest-neighbor Fe atoms. Also, the sites 4, 5, and 6 with 28.5, 24.7, and 13.9 T are the (A,C) or (B,D) sites with six-, five-, and three-nearest-neighbor Fe atoms, respectively. Finally, the site 7 is regarded as the site that has less than three neighboring Fe atoms with a small hyperfine magnetic field of less than 5 T. By the fitting of the experimental data with these seven sites, we obtain information on local magnetic environments of the Fe atoms in the epitaxial  $\text{Fe}_{3+x}\text{Si}_{1-x}$  films on Ge(111). Note that the filling quadrupole shift was fixed to zero, since it is reported to be negligible in bulk  $\text{Fe}_3\text{Si}$ .<sup>28</sup>

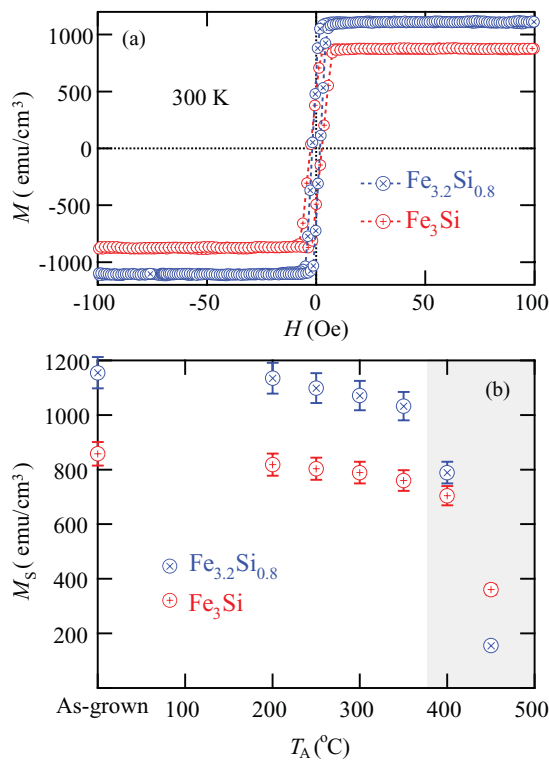


FIG. 3. (Color online) (a)  $M-H$  curves at 300 K for as-grown  $\text{Fe}_3\text{Si}$  (red) and  $\text{Fe}_{3.2}\text{Si}_{0.8}$  (blue) films. (b)  $M_S$  as a function of  $T_A$  for  $\text{Fe}_3\text{Si}$  (red) and  $\text{Fe}_{3.2}\text{Si}_{0.8}$  (blue) films.

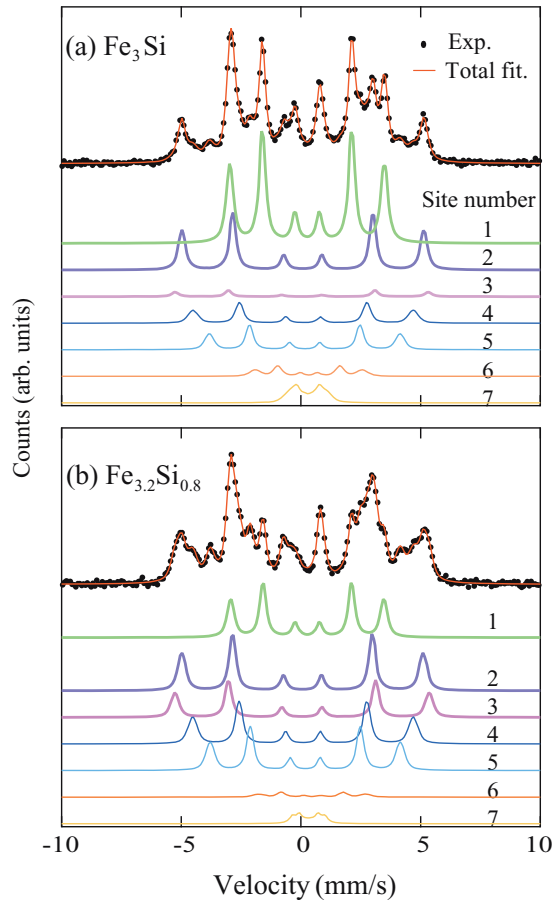


FIG. 4. (Color online) The  $^{57}\text{Fe}$  Mössbauer spectra (solid circles) of as-grown (a)  $\text{Fe}_3\text{Si}/\text{Ge}(111)$  and (b)  $\text{Fe}_{3.2}\text{Si}_{0.8}/\text{Ge}(111)$  at room temperature, together with seven fitting curves as denoted in the text.

The percentage of the fitted area versus site number for as-grown  $\text{Fe}_3\text{Si}$  and  $\text{Fe}_{3.2}\text{Si}_{0.8}$  films is presented in Fig. 5, together with that for the postannealed films. The effect of the postannealing on the local magnetic environments will be discussed in the next section. If we fabricate a perfectly  $\text{D0}_3$ -ordered  $\text{Fe}_3\text{Si}$  film, we should obtain 66.6% for the site 1 and 33.3% for the site 2.<sup>15,28,32</sup> For the as-grown  $\text{Fe}_3\text{Si}$  film, the fitting results show that site 1:site 2 = 44.2%:22.4%, indicating that the local degree of the  $\text{D0}_3$  ordering can be estimated to be  $\sim 67\%$ . The hyperfine magnetic field and isomer shifts relative to  $\alpha$ -Fe of Fe(I) and Fe(II) are estimated to be 20.0 T and 0.26 mm/s and 31.3 T and 0.08 mm/s, respectively. These values are consistent with those reported in literature.<sup>15,28,32</sup> Furthermore, the site 3 is less than 2.5% of all the detected magnetic environments around the Fe sites. From these results, when the chemical composition is stoichiometric ( $x = 0$ ), relatively high amounts of the  $\text{D0}_3$ -ordered structure can be formed despite the growth at such a low temperature of 130 °C. The degree of the ordering of our as-grown  $\text{Fe}_3\text{Si}$  films is close to the low-temperature grown epitaxial  $\text{Fe}_3\text{Si}$  films on GaAs(001) reported recently by Jenichen *et al.*<sup>9</sup> They found that 30% of Si atoms is exchanged with the Fe atoms of the (A,C) site even for the nearly stoichiometric films.<sup>9</sup> Considering the facts for the  $\text{Fe}_3\text{Si}$  film on GaAs(001), we can speculate that the main origin of the disorder for our as-grown  $\text{Fe}_3\text{Si}$  films is the site

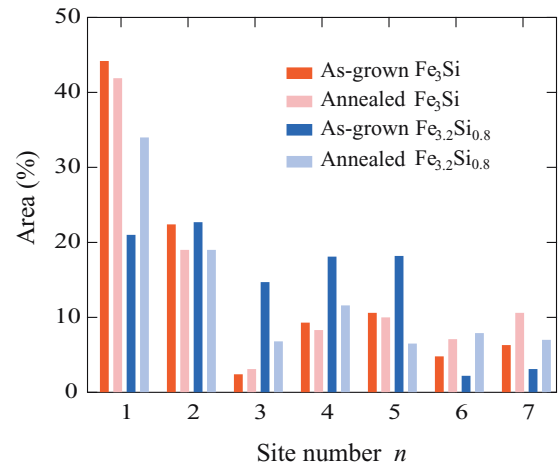


FIG. 5. (Color online) Fitted area vs site number for various samples, estimated by CMES measurements and best fitting. The sites 1 and 2 correspond to Fe(I) and Fe(II), shown in Fig. 1, for the ideal  $\text{D0}_3$ -ordered  $\text{Fe}_3\text{Si}$ .

occupation of Si atoms with the (A,C) sites, which can explain the increase in the percentage of the sites 4, 5, and 6 shown in Fig. 5. It should be noted that the local degree of the structural ordering of  $\text{Fe}_3\text{Si}$  thin film on a group-IV semiconductor can be estimated and its value reaches  $\sim 67\%$ .

For the as-grown  $\text{Fe}_{3.2}\text{Si}_{0.8}$  film, on the other hand, we can see a marked reduction in the percentage of the area fitted with the site 1 and enhancement in that with the site 3, together with the sites 4 and 5. Furthermore, there is almost no variation in the site 2 compared to the stoichiometric  $\text{Fe}_3\text{Si}$  film. In the previous study of epitaxial  $\text{Fe}_{3.34}\text{Si}_{0.66}$  films on GaAs(001),<sup>9</sup> Jenichen *et al.* have already revealed that Si atoms can occupy the (A,C) sites and that there is almost no  $\text{D0}_3$ -ordered structure.<sup>9</sup> Namely, when the chemical composition of the LTMBE-grown  $\text{Fe}_{3+x}\text{Si}_{1-x}$  films is Fe-rich off-stoichiometry, the site selection preference can not be realized. Also, it is well known that excess Fe atoms can easily occupy the D site.<sup>22</sup> As shown in Fig. 2(b), since we do not obtain  $\text{D0}_3$ -ordered structures, almost the same situations that Jenichen *et al.* found can be assumed for the as-grown  $\text{Fe}_{3.2}\text{Si}_{0.8}$  film. Thus, the enhancement in the percentage of the site 3 indicates that excess Fe atoms occupied the D site surrounded by Fe atoms occupying the (A,C) sites. Simultaneously, Fe(I)-like Fe atoms are reduced by the decrease in Si nearest neighbors, causing the marked reduction in that of the site 1. As mentioned above, when the exchange of Si atoms of the D site for Fe atoms of the (A,C) sites is increased, the Fe atoms surrounded by six or five Fe atoms are increased, showing the enhancement in that of the sites 4 and 5.

Considering the site occupation of Fe atoms, we can explain the difference in  $M_S$  between as-grown  $\text{Fe}_3\text{Si}$  and  $\text{Fe}_{3.2}\text{Si}_{0.8}$  films shown in Fig. 3. When the chemical composition deviates from the stoichiometric to the Fe-rich off-stoichiometric chemical compositions, the nearest-neighbor Si atoms for the site-occupied Fe atoms are decreased, leading to an enhancement in the net magnetic moments.<sup>28-32</sup> By analyzing  $^{57}\text{Fe}$  Mössbauer spectra, we can clearly understand that  $M_S$  for  $\text{Fe}_{3.2}\text{Si}_{0.8}$  films is always larger than that for  $\text{Fe}_3\text{Si}$  films despite the increase in the disordered phases. In order to fabricate

highly ordered films on Ge(111), one should conduct careful and precise control of the chemical composition of the ratio of Fe to Si by using Knudsen cells during the low-temperature growth. We also infer that the precise control of the chemical composition is the most important factor for low-temperature-grown Heusler compounds on Si(111) or Ge(111) to achieve highly ordered crystal structures.<sup>7,8,13,14,17,21</sup>

## VI. EFFECT OF POSTANNEALING

We discuss the effect of the postannealing on the structural ordering for both  $\text{Fe}_3\text{Si}$  and  $\text{Fe}_{3.2}\text{Si}_{0.8}$  films. As described in Fig. 3(b), we have confirmed the slight reduction in  $M_S$  from  $\sim 858$  and  $\sim 1155$   $\text{emu}/\text{cm}^3$  to  $\sim 760$  and  $\sim 1033$   $\text{emu}/\text{cm}^3$  for  $\text{Fe}_3\text{Si}$  and  $\text{Fe}_{3.2}\text{Si}_{0.8}$ , respectively, after the post annealing at  $T_A = 350$  °C. Since we could not observe marked changes in the structural quality in the vicinity of the interface by TEM, NED, and Rutherford backscattering spectroscopy (RBS) measurements,<sup>13,14</sup> we considered that the origin of the reduction in  $M_S$  is not due to the increase in the structural disorder near the interface but is due to the other intrinsic phenomena. Here, we want to go back to the results of the site occupation in Fig. 5. By the comparison of before and after annealing for  $\text{Fe}_3\text{Si}$  films (stoichiometric composition), we see small changes in the fitted area for all the sites. In particular, the site 7 is slightly increased but the sites 1 and site 2 are decreased. This means that the postannealing does not improve the degree of the structural ordering, but small unexpected position changes in Fe atoms are induced. In the past study reported by Miyazaki *et al.*,<sup>32</sup> the disordered structure in nearly stoichiometric  $\text{Fe}_{2.85}\text{Si}_{1.15}$  films grown on crystallized-glass substrates did not transform to the  $\text{D0}_3$ -ordered structure even after the postannealing at 500 or 700 °C, similar to our results for stoichiometric  $\text{Fe}_3\text{Si}$  films. The precise origin is now under discussion, but this structural stabilization arising from the stoichiometric chemical composition may affect indirectly the increase in the percentage of the site 7 by the postannealing. We infer that the increase in the site 7 after the annealing originates from an atomic interdiffusion, which we could not detect by the other structural analyses at the  $\text{Fe}_3\text{Si}/\text{Ge}$  interface. This phenomenon can lead to the reduction in  $M_S$ , as shown in Fig. 3(b).

In contrast, for  $\text{Fe}_{3.2}\text{Si}_{0.8}$  films (off-stoichiometric composition), we can clearly see the significant changes in the fitted area after the annealing. The percentage of the site 1 is markedly enhanced while those of the sites 3, 4, and 5 are decreased. The results show that site 1:site 2 = 34.0%:19.0%, indicating the local degree of the structural ordering of  $\sim 53\%$ . Namely, we can dramatically recover  $\text{D0}_3$ -ordered structures by using postannealing for the off-stoichiometric  $\text{Fe}_{3.2}\text{Si}_{0.8}$  film. This feature is also consistent with that of off-stoichiometric  $\text{Fe}_{3.4}\text{Si}_{0.6}$  films on crystallized-glass substrates.<sup>32</sup> As discussed in the previous section, it is inferred that there are many Si atoms of the (A,C) sites and Fe atoms of the D site. After the annealing, the Fe atoms occupying the D site can be exchanged for Si atoms occupying the (A,C) sites, causing an increase in the amount of  $\text{D0}_3$ -ordered phases. Also, if there are some vacancies at the (A,C) sites because of low-temperature and Fe-rich growth conditions, the Fe atoms

occupying the D site can move to the (A,C) sites, also leading to the increase in the amount of  $\text{D0}_3$ -ordered phases. With recovering the  $\text{D0}_3$  ordering, the relative increase in the nearest-neighbor Si atoms induces the reduction in the local magnetic moments of the Fe atoms at the (A,C) sites. This scenario is quite reasonable to explain the experimental results showing gradual reduction in  $M_S$  [Fig. 3(b)] by the postannealing.<sup>14</sup> In addition, since the sites 6 and 7, which are attributed to three- or less-than-three-nearest-neighbor Fe atoms, increase simultaneously, the unexpected atomic interdiffusion at the  $\text{Fe}_3\text{Si}/\text{Ge}$  interface should be considered at least.

We have performed a qualitative discussion of the effect of the postannealing on the structural ordering for low-temperature-grown epitaxial  $\text{Fe}_{3+x}\text{Si}_{1-x}$  films on Ge(111). However, there are some unclear features as follows. In the past studies,<sup>33–35</sup> Fe-diffusion phenomena in bulk  $\text{Fe}_{3+x}\text{Si}_{1-x}$  with stoichiometry and off-stoichiometry were experimentally and theoretically investigated. For bulk samples with high-temperature annealing ( $T_A = 720 \sim 900$  °C), the Fe diffusion depended strongly on the chemical composition. In general, the Fe atoms can jump predominantly via vacancies on the (A,C) and B sites for stoichiometric  $\text{Fe}_3\text{Si}$ , while the Fe jumps can occur mainly via vacancies on the D site for Fe-rich off-stoichiometric  $\text{Fe}_{3+x}\text{Si}_{1-x}$ .<sup>33</sup> This means that the diffusivity of the Fe atoms for stoichiometric  $\text{Fe}_3\text{Si}$  is much higher (a factor of 5 to 10) than that for Fe-rich off-stoichiometric  $\text{Fe}_{3+x}\text{Si}_{1-x}$ .<sup>33–35</sup> This knowledge for the bulk samples with high-temperature annealing is quite different from our results. At least, since evident restoration of the  $\text{D0}_3$ -ordered structure can be seen only for the off-stoichiometric  $\text{Fe}_{3.2}\text{Si}_{0.8}$  film, we can not easily take into account the same mechanism such as Fe jumps between the sites observed for the bulk samples. We note that the effect of the postannealing on the structural ordering for our epitaxial  $\text{Fe}_{3+x}\text{Si}_{1-x}$  films is similar to that for sputtered  $\text{Fe}_{3+x}\text{Si}_{1-x}$  films.<sup>32</sup> Thus, we consider that the observed features after the annealing may occur only for the thin-film samples. Recently, the depth dependence of the Fe diffusion in  $\text{Fe}_{3+x}\text{Si}_{1-x}$  thin films by the annealing was studied by Kmiec *et al.*,<sup>36</sup> and they cleared that the Fe diffusivity is enhanced at the surface and is continuously decreased with the sample depth. Therefore, understanding of the effect of film thickness on the structural ordering induced by the postannealing is important for thin-film samples. Furthermore, since the vacancy formation enthalpies can depend on the chemical composition,<sup>37</sup> we should also consider the influence of the vacancies at the (A,C) and B sites for thin-film samples.

## VII. CONCLUSION

We have examined the local structural ordering of epitaxial  $\text{Fe}_3\text{Si}$  and  $\text{Fe}_{3.2}\text{Si}_{0.8}$  films on Ge(111) grown at a very low temperature of 130 °C. Despite thin-film samples on semiconductor substrates, the site occupation of the Fe atoms for both stoichiometric and off-stoichiometric films can be discussed by analyzing their  $^{57}\text{Fe}$  Mössbauer spectra. In consequence, a relatively high degree of the  $\text{D0}_3$  ordering can be quantitatively obtained only for the stoichiometric film even in as-grown conditions (130 °C). We also found that the

postannealing can act effectively on the improvement of the structural ordering only for the off-stoichiometric films.

### ACKNOWLEDGMENTS

K.H. and M.M. thank Y. Maeda for useful discussions. This work was partly supported by Industrial Technology Research

Grant Program from NEDO, Precursory Research for Embryonic Science and Technology (PRESTO) from JST, and Core Research for Evolutional Science and Technology (CREST) from JST. The Mössbauer measurements were supported by the Nanotechnology Network Project of MEXT, Japan.

\*hamaya@ed.kyushu-u.ac.jp

- <sup>1</sup>V. A. Niculescu, T. J. Burch, and J. I. Budnick, *J. Magn. Magn. Mater.* **39**, 223 (1983).
- <sup>2</sup>A. Ionescu, C. A. F. Vaz, T. Trypiniotis, C. M. Gürtler, H. García-Miquel, J. A. C. Bland, M. E. Vickers, R. M. Dalgliesh, S. Langridge, Y. Bugoslavsky, Y. Miyoshi, L. F. Cohen, and K. R. A. Ziebeck, *Phys. Rev. B* **71**, 094401 (2005).
- <sup>3</sup>J. Herfort, H.-P. Schönherr, and K. H. Ploog, *Appl. Phys. Lett.* **83**, 3912 (2003).
- <sup>4</sup>J. Herfort, H.-P. Schönherr, K.-J. Friedland, and K. H. Ploog, *J. Vac. Sci. Technol. B: Microelectron. Process. Phenom.* **22**, 2073 (2004).
- <sup>5</sup>T. Yoshitake, D. Nakagauchi, T. Ogawa, M. Itakura, N. Kuwano, Y. Tomokiyo, T. Kajiwara, and K. Nagayama, *Appl. Phys. Lett.* **86**, 262505 (2005).
- <sup>6</sup>K. Kobayashi, T. Sunohara, M. Umada, H. Yanagihara, E. Kita, and T. Suemasu, *Thin Solid Films* **508**, 78 (2006).
- <sup>7</sup>K. Hamaya, K. Ueda, K. Kasahara, Y. Ando, T. Sadoh, and M. Miyao, *Appl. Phys. Lett.* **93**, 132117 (2008).
- <sup>8</sup>T. Sadoh, M. Kumano, R. Kizuka, K. Ueda, A. Kenjo, and M. Miyao, *Appl. Phys. Lett.* **89**, 182511 (2006); K. Ueda, Y. Ando, M. Kumano, T. Sadoh, Y. Maeda, and M. Miyao, *Appl. Surf. Sci.* **254**, 6215 (2008); M. Miyao *et al.*, *Thin Solid Films* **518**, S273 (2010).
- <sup>9</sup>B. Jenichen, V. M. Kaganer, J. Herfort, D. K. Satapathy, H.-P. Schönherr, W. Braun, and K. H. Ploog, *Phys. Rev. B* **72**, 075329 (2005).
- <sup>10</sup>K. Lenz, E. Kosubek, K. Baberschke, H. Wende, J. Herfort, H.-P. Schönherr, and K. H. Ploog, *Phys. Rev. B* **72**, 144411 (2005).
- <sup>11</sup>H. Vinzelberg, J. Schumann, D. Elefant, E. Arushanov, and O. G. Schmidt, *J. Appl. Phys.* **104**, 093707 (2008).
- <sup>12</sup>D. Berling, P. Bertoncini, M. C. Hand, A. Mehdaoui, C. Pirri, P. Wetzel, G. Gewinner, and B. Loegel, *J. Magn. Magn. Mater.* **212**, 323 (2000).
- <sup>13</sup>Y. Maeda, T. Jonishi, K. Narumi, Y. Ando, K. Ueda, M. Kumano, T. Sadoh, and M. Miyao, *Appl. Phys. Lett.* **91**, 171910 (2007).
- <sup>14</sup>Y. Ando, K. Hamaya, K. Kasahara, K. Ueda, Y. Nozaki, T. Sadoh, Y. Maeda, K. Matsuyama, and M. Miyao, *J. Appl. Phys.* **105**, 07B102 (2009).
- <sup>15</sup>B. Krumme, C. Weis, H. C. Herper, F. Stromberg, C. Antoniak, A. Warland, E. Schuster, P. Srivastava, M. Walterfang, K. Fauth, J. Minár, H. Ebert, P. Entel, W. Keune, and H. Wende, *Phys. Rev. B* **80**, 144403 (2009).
- <sup>16</sup>M. Hashimoto, J. Herfort, H.-P. Schönherr, and K. H. Ploog, *Appl. Phys. Lett.* **87**, 102506 (2005); M. Hashimoto, J. Herfort, A. Trampert, and K. H. Ploog, *J. Cryst. Growth* **301–302**, 592 (2007).
- <sup>17</sup>K. Ueda, K. Hamaya, K. Yamamoto, Y. Ando, T. Sadoh, Y. Maeda, and M. Miyao, *Appl. Phys. Lett.* **93**, 112108 (2008); K. Hamaya, H. Itoh, O. Nakatsuka, K. Ueda, K. Yamamoto, M. Itakura, T. Taniyama, T. Ono, and M. Miyao, *Phys. Rev. Lett.* **102**, 137204 (2009); S. Yamada, K. Ueda, K. Yamamoto, K. Hamaya, T. Sadoh, and M. Miyao, *Thin Solid Films* **518**, S278 (2010); S. Yamada, K. Hamaya, K. Yamamoto, T. Murakami, K. Mibu, and M. Miyao, *Appl. Phys. Lett.* **96**, 082511 (2010); K. Kasahara, K. Yamamoto, S. Yamada, T. Murakami, K. Hamaya, K. Mibu, and M. Miyao, *J. Appl. Phys.* **107**, 09B105 (2010).
- <sup>18</sup>M. Zander, J. Herfort, K. Kumakura, H.-P. Schönherr, and A. Trampert, *J. Phys. D: Appl. Phys.* **43**, 305004 (2010).
- <sup>19</sup>J. M. Gallego, J. M. Garcia, J. Alvarez, and R. Miranda, *Phys. Rev. B* **46**, 13339 (1992).
- <sup>20</sup>A. Filipe, A. Schuhl, and P. Galtier, *Appl. Phys. Lett.* **70**, 129 (1997).
- <sup>21</sup>Y. Ando, K. Hamaya, K. Kasahara, Y. Kishi, K. Ueda, K. Sawano, T. Sadoh, and M. Miyao, *Appl. Phys. Lett.* **94**, 182105 (2009); Y. Ando, K. Kasahara, Y. Enomoto, K. Yamane, K. Hamaya, K. Sawano, T. Kimura, and M. Miyao, *Appl. Phys. Express* **3**, 093001 (2010).
- <sup>22</sup>W. A. Hines, A. H. Menotti, J. I. Budnick, T. J. Burch, T. Litenta, V. Niculescu, and K. Raj, *Phys. Rev. B* **13**, 4060 (1976).
- <sup>23</sup>J. Kudrnovský, N. E. Christensen, and O. K. Andersen, *Phys. Rev. B* **43**, 5924 (1991).
- <sup>24</sup>S. Fujii, S. Ishida, and S. Asano, *J. Phys. Soc. Jpn.* **64**, 185 (1995).
- <sup>25</sup>E. G. Moroni, W. Wolf, J. Hafner, and R. Podloucky, *Phys. Rev. B* **59**, 12860 (1999).
- <sup>26</sup>A. Bansil, S. Kaprzyk, P. E. Mijnaerends, and J. Tobola, *Phys. Rev. B* **60**, 13396 (1999).
- <sup>27</sup>N. I. Kulikov, D. Fristot, J. Hugel, and A. V. Postnikov, *Phys. Rev. B* **66**, 014206 (2002).
- <sup>28</sup>M. B. Stearns, *Phys. Rev.* **129**, 1136 (1963).
- <sup>29</sup>T. Shinjo, Y. Nakamura, and N. Shikazono, *J. Phys. Soc. Jpn.* **18**, 797 (1963).
- <sup>30</sup>M. B. Stearns, *Phys. Rev. B* **4**, 4069 (1963).
- <sup>31</sup>T. J. Burch, T. Litenta, and J. I. Budnick, *Phys. Rev. Lett.* **33**, 421 (1974).
- <sup>32</sup>M. Miyazaki, M. Ichikawa, T. Komatsu, and K. Matusita, *J. Appl. Phys.* **71**, 2368 (1992).
- <sup>33</sup>B. Sepiol and G. Vogl, *Phys. Rev. Lett.* **71**, 731 (1993).
- <sup>34</sup>B. Sepiol, A. Meyer, G. Vogl, R. Rüfer, A. I. Chumakov, and A. Q. R. Baron, *Phys. Rev. Lett.* **76**, 3220 (1996).
- <sup>35</sup>S. Dennler and J. Hafner, *Phys. Rev. B* **73**, 174303 (2006).
- <sup>36</sup>D. Kmiec, B. Sepiol, M. Sladeczek, M. Rennhofer, S. Stankov, G. Vogl, B. Laenens, J. Meersschaut, T. Ślęzak, and M. Zajkaç, *Phys. Rev. B* **75**, 054306 (2007).
- <sup>37</sup>E. A. Kümmerle, K. Badura, B. Sepiol, H. Mehrer, and H.-E. Schaefer, *Phys. Rev. B* **52**, R6947 (1995).